NUMERICAL INVESTIGATION OF A LAYERED HYBRID LOAD INTRODUCTION ELEMENT FOR THIN-WALLED CFRP STRUCTURES

Alexander Herwig[1], Carsten Schmidt[2] and Peter Horst[1]

[1]Institute of Aircraft Design and Lightweight Structures, Technische Universität Braunschweig, Ottenbecker Damm 12, Germany, al.herwig@tu-braunschweig.de, www.tu-braunschweig.de/ifl
[2]Institute of Production Engineering and Machine Tools, Leibniz Universität Hannover, Ottenbecker Damm 12, Germany schmidt_c@ifw.uni-hannover.de, www.hpcfk.de

Keywords: fiber-metal laminate, insert, embedded load introduction, joints

Abstract
The project "Multi-Layer Inserts" (MLI) proposes a new design for inserts used in thin-walled structures made of carbon fiber reinforced plastic (CFRP). The proposed insert consists of multiple thin metal sheets and is build up simultaneously with the laminate in a fully automated intrinsic hybridization process, eliminating time-consuming post-processing steps. Furthermore, such inserts significantly increase the bonding area between metal and CFRP in comparison to conventional inserts at equal weight. This results in a significant increase of the loads that can be transmitted into the CFRP.
The individual material layers of the local CFRP-metal-hybrid (CFRP, metal, adhesive) are very thin and form a multitude of adhesive connections. Prior investigations have shown advantages of octagonal shaped metal inserts in reducing strain concentrations. The present work discusses a simplification methodology to investigate the MLI's dependence on and sensitivity to design parameters by dividing the model of the complex adhesive connection into combinations of common lap joints. After proving the transferability of the lap joint approach for very thin laminates, a comparison of the experimentally measured surface strain distribution near an octagonal MLI is used to assess the quality of the approximation.

1. Introduction
The project "Multi-Layer Inserts" (MLI) proposes a new design for inserts used in thin-walled structures made of carbon fiber reinforced plastic (CFRP). The proposed insert consist of multiple thin metal sheets and is build up simultaneously with the laminate in a fully automated intrinsic hybridization process, eliminating time-consuming post-processing steps [1]. Furthermore, such inserts significantly increase the bonding area between metal and CFRP in comparison to conventional inserts at equal weight. This results in a significant increase of the loads that can be transmitted into the CFRP. The detailed positioning of a single metal sheet in the laminate layers is shown in Figure 1.
The individual material layers of the local CFRP-metal-hybrid (CFRP, metal, adhesive) are very thin, i.e. 0.1 mm up to 1.34 mm and form a multitude of adhesive connections as can be seen in Figure 1. Strain concentrations occur in both material transitions A and B, whereby it turns out that at transition B the increase of the strain in the upper and lower CFRP layer is the sizing factor of the current design. The design process of a MLI has to differentiate two load scenarios: The load introduction directly into the MLI and the transmission of structural loads through the MLI. The complexity of their interaction prevents the application of analytical calculation methods. However, when modelling thin layers in finite element analysis, the numerical effort is significantly increased due to the large number of elements due to their allowed aspect ratio. The present work considers the MLI as an inclusion, which is obstructing the load transition within the structure and discusses a methodology to investigate its dependence on

and sensitivity to design parameters in order to approximate the resulting strain field and especially the strain concentrations.

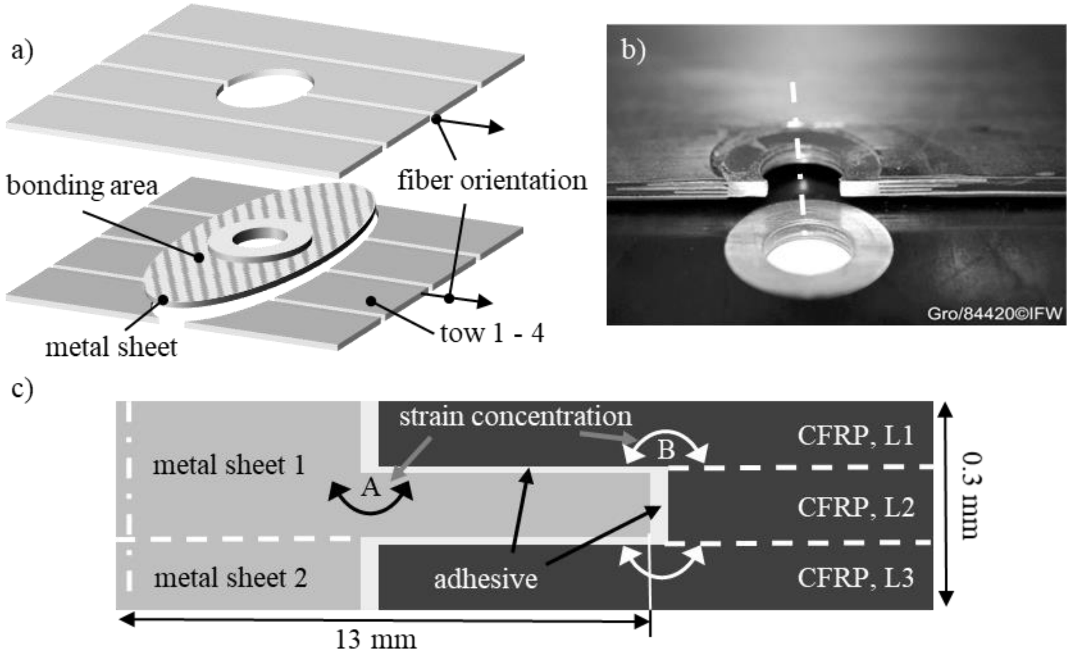

Figure 1: a) Schematic view of a double-layer laminate with (MLI-) metal sheet b) Cross section of MLI with center hole [1] c) Simplified model with failure critical areas A (single-lap + butt joint) and B (double-lap + butt joint).

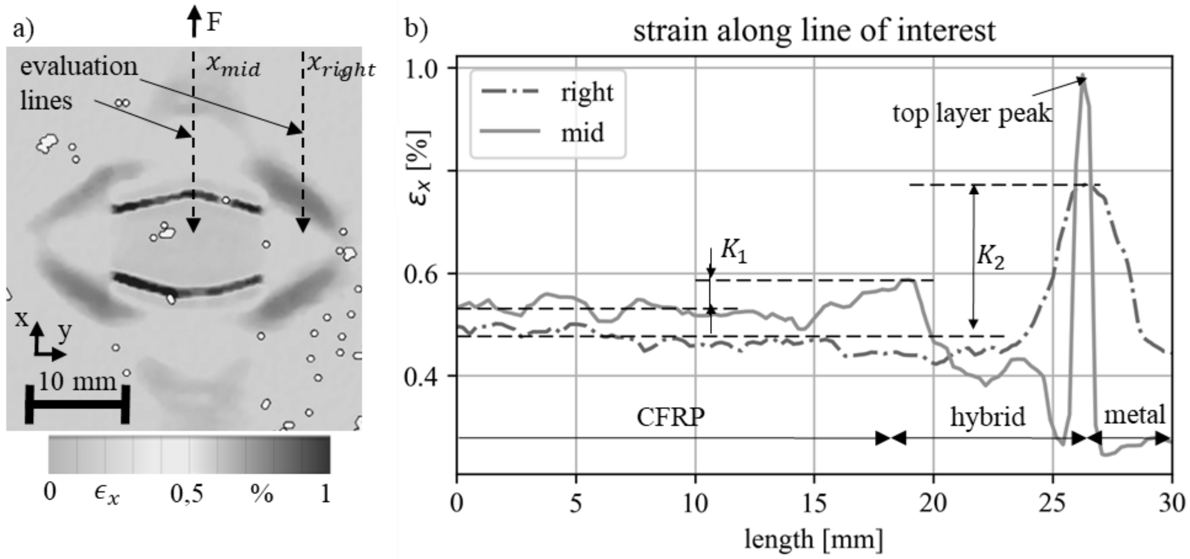

Figure 2: a) Surface strain measurement of a multi-layer insert in a cross laminate with decagonal metal sheets [2] b) Strain component ϵ_x with concentrations factors $K_1 = 1.1$ and $K_2 = 1.62$ along the evaluation lines.

Figure 2a shows the strain distribution in load direction (ϵ_x) at the surface of the top layer of a laminate with a MLI build by octagonal metal sheets, while the detailed strain values along the depicted evaluation lines are shown in Figure 2b. The strain concentrations at the transitions from steel to the surrounding CFRP are clearly visible. Edges in fiber direction show no elevated strain, while the tips of the metal sheets in fiber direction show reduced strain in comparison to the clearly visible high strain at the outer 32°-edges. The geometry parameters as well as the division of the complex adhesive connection into subsections is shown in Figure 3. The outward located section C is characterized by a continuous CFRP top and bottom layer, while the CFRP layer in the center section D is continued by a metal sheet. However, by only considering one layer at a time the section can be represented as a simplified common joint element such as single-lap, double-lap or butt joints [3] (see Figure 4).

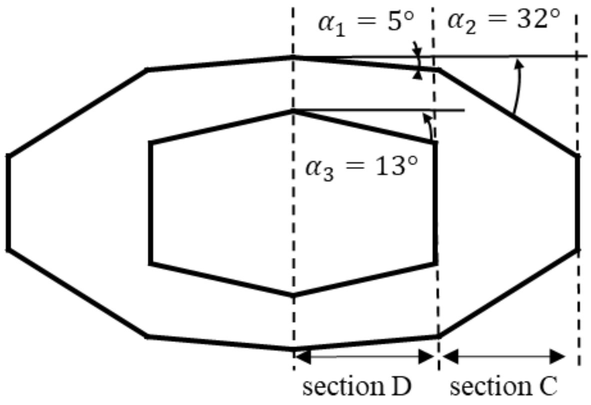

Figure 3: Sectioning and transition angles of the decagonal metal sheet.

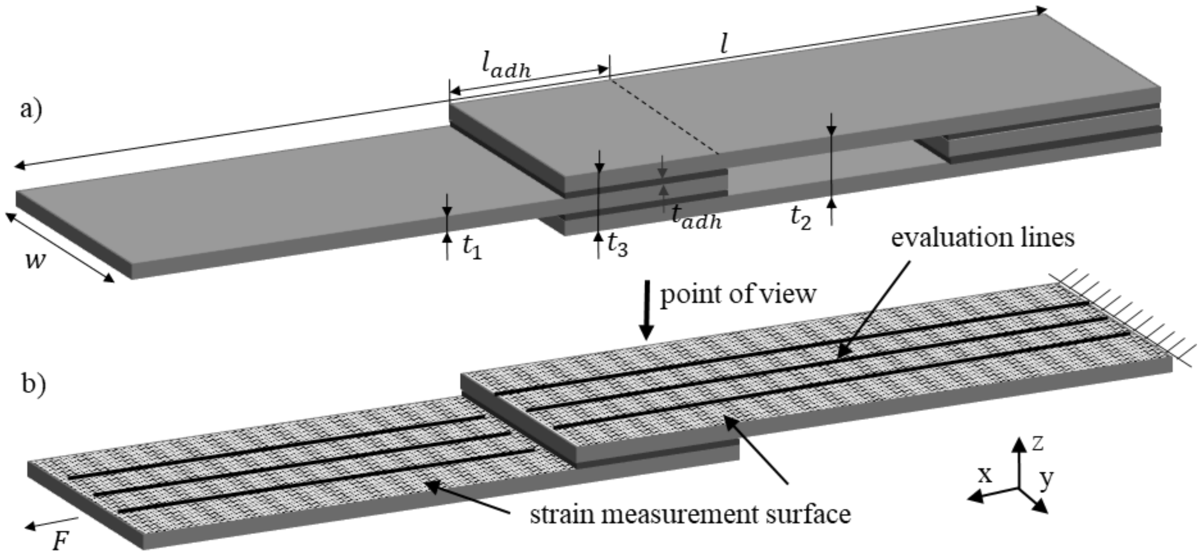

Figure 4: a) Geometrical parameters of the investigated double-lap joint b) Load case, point of view and surface for the strain measurement via digital image correlation (DIC).

Lap joints are the simplest and commonly used adhesive joining techniques. Volkersen [4] published an analytical description of an adhesive joint as early as 1938. Based on this work several terms were added e.g. to account for a stress gradient in thickness direction or to allow shear deformations in the adherend [5,6]. This investigation also uses Volkersens simplification neglecting the adherend shear since the actual error in the application on very thin layers should be neglectable. Therefore, the presented results can be seen as conservative estimates that should not be exceeded by other results. To prove the applicability of the analytical model and the presented FE-approach for very thin laminates, the calculated strain values are compared to the surface strain measured by digital image correlation (DIC). Therefore, three sets of specimens are produced: The first set corresponds to thin double-lap joint specimen with a rectangular adhesive surface (see Figure 4) used as model validation. The second and third set with angled adhesive surfaces and therefore also angled metal sheets (see Figure 5) are produced with a continuous top and bottom layer (type C) and with a disturbed top and bottom layer (type D) in order to investigate the influence of the shape of the adhesive surface.

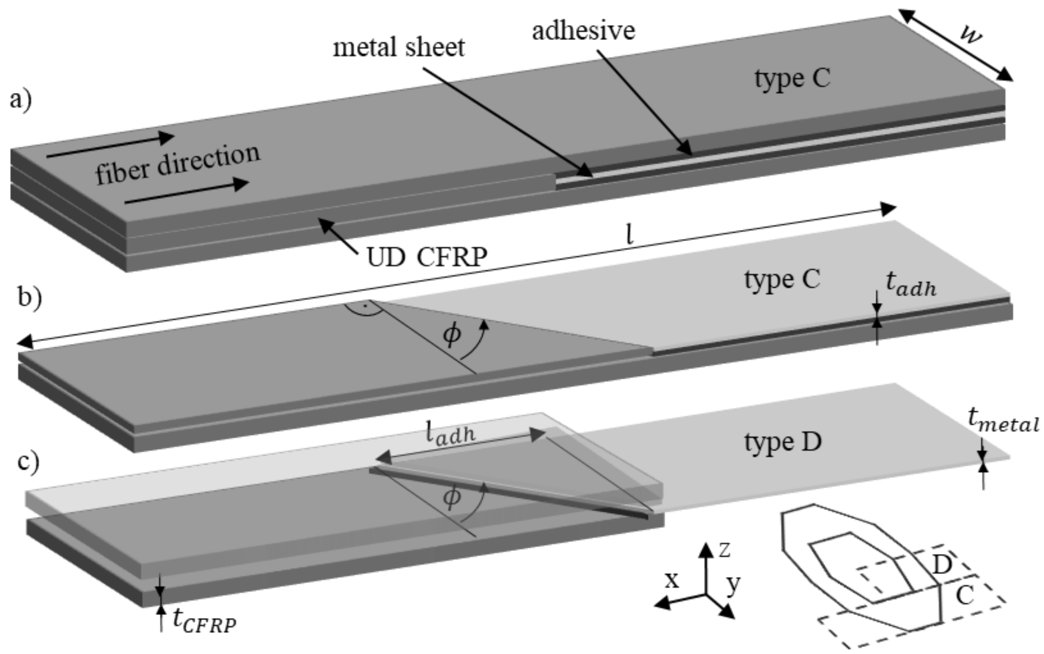

Figure 5: a) Modified angular lap joint with an angled metal sheet and continuous top and bottom layers b) cross section in the XY-plane of the specimen defining the transition angle ϕ c) geometry of specimen type D with a discontinuous top and bottom layer.

Specimen preparation

All specimen are manufactured by a hand laminating process using Cycom 977-2-35-12KHTS-134-300 preimpregnated fiber tapes (prepregs) as adherend material and 3M 163-2 as adhesive, which is supplied on a non-woven supporting carrier. The thickness of the prepregs is 0.134 mm before and 0.1 mm after curing at $T_{cur} = 180°$ and $p = 10$ bar. The adhesive thickness after curing is 0.18 mm. The material properties and investigated geometry parameters can be taken from Table 1 and Table 2

Table 1: Parameters of the materials used in this investigation.

	E_1 (GPa)	E_2 (GPa)	ν_{21} (-)	ν_{22} (-)	G_{21} (GPa)
Cycom 977-2	117.3	9.1	0.27	0.37	4.2
AF163-2	1.1	-	0.34	-	-

Table 2: Geometrical parameters of the double-lap joint and validation specimen.

	Thickness t [mm]	Length l [mm]	Width w [mm]	Overlap length l_{adh} [mm]
metal / CFRP / adhesive	0.1 / 0.15 / 0.18	200	25	25

The measurement of the surface strain is performed with an ARAMIS 12M system and takes place at the surface depicted in Figure 4b with a frequency of 3 Hz during tensile testing. Especially the localized strain concentrations at the edges of the adhesive joints are of interest. The measuring volume is calibrated to 65 x 49 mm with a facet size of 22 pixels and an 18 pixel distance between the two facet centers, which corresponds approximately to 0.33 mm at the specimen surface. Facets positioned at material transitions or steps are especially warped and lead to an overestimation of the local strain values, therefore a median filter involving the two neighbor facets in each direction is used to smooth the strain values.

FE Model of a double-lap joint

Several descriptions and experimental investigations of lap joints with isotropic adherends already exist; the earliest are by Volkersen [4] describing the shear strain in the adhesive layer. Tsai et al. [5] also measures the strain in the individual FRP layers by moiré interferometry in symmetric double-lap joints, while more recently Gültekin et al. [7] compared the experimental failure loads of asymmetrical aluminum/CFRP single-lap joints with FE computations. All these computations were performed in two dimensions, thus cannot consider effects resulting from the material transition shape in the XY-Plane. The generated FE mesh for the present model validation is shown in Figure 6. To accurately describe the strain in the material transitions the mesh size in this area is at least reduced by an order of magnitude as suggested by Gültekin.

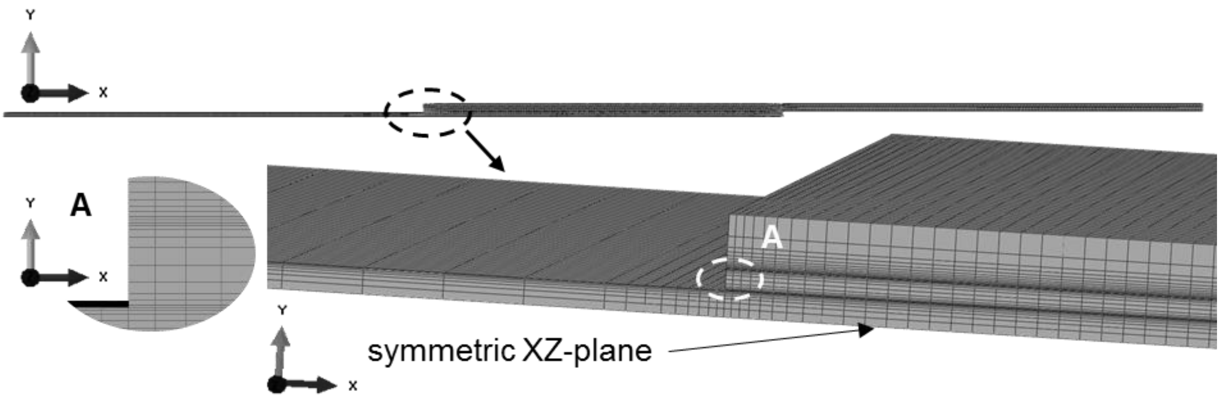

Figure 6: FE mesh of double-lap joint. Thickness of adhesive 0.18 mm and an adherend thickness of 0.45 mm. The element size at the material transitions is reduced to a thickness of 0.006 mm.

Results for a regular double-lap joint

The global strain as well as the strain values along the evaluation lines depicted in Figure 4b are compared. The measured and calculated strain on the specimen surface are shown in Figure 7. Apart from the transition into the single adherend, the strain values match each other very well. It can be assumed, that the deviation of the raw DIC strain values is caused by the finite measuring distance between the facets in combination with the localized strain and the step in thickness direction, which warps the facets even further. In order to obtain a continuous strain the following values are filtered by a median filter over the two adjoining values. The results suggest that the effects in double-lap joints can be calculated in such simplified FE models and match the measured strain values of the DIC.

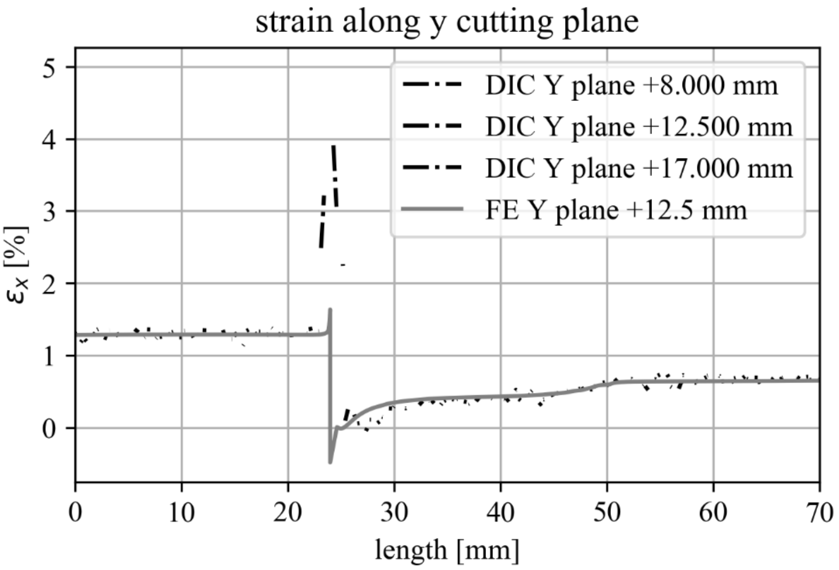

Figure 7: Comparison between the raw strain values measured by digital image correlation (DIC) and the FE-results on the surface of a DLJ specimen with CFRP adherends, t=0.1 mm.

Angular lap joints

The two load cases have to be examined: Type C with a continuous top and bottom layer and type D with an interrupted CFRP layer. The specimens are prepared as three layered unidirectional laminates, whereby the middle layer is partly replaced by metal sheet as shown in Figure 5.

In order to increase the volume of the transition area which is proportional to $V \sim \cos(\phi)^{-1}$[8] the transition is performed under an angle ϕ. When performed in thickness direction this approach leads to a strain reduction in lap joints and has already been widely used for example in scarfed FRP repair patches [9].

Type C – continuous top and bottom layer

Figure 8a shows an exemplary strain distribution along the angled metal CFRP transition for a 45° angle, while Figure 8b depicts the strain along the evaluation lines. In order to investigate the dependence of the transition angle the ratio between the strain peak and the mean strain (see Figure 8b) are calculated. The measured strain along the transition as well as the calculated ratios $K_3 = 1.42$, $K_4 = 1.4$, $K_5 = 1.4$ are nearly constant therefore they also could be calculated by a 2D analytical as well as a 2D FE model. Additionally Figure 8c shows very little decline in the ratio between the mean strain before and the maximum in the transition. Therefore, the strain ratio in the transition can be considered independent from the transition angle.

Type D – disturbed top and bottom layer

Figure 9a show and exemplary strain distribution of the ϵ_x strain component for a transition angle of $\phi = 45°$. Figure 9b shows the values along the evaluation lines. In contrast to specimen type C the strain in the transition is not constant but elevated at the beginning convergence to a constant value as the distance between the CFRP and metal endings increase. This is also visible in the strain ratios $K_6 = 1.15$, $K_7 = 1.23$, $K_8 = 1.41$ which converging to same ration of approximately $K = 1.4$ as specimen type C. The distance between the metal and CFRP endings can therefore be seen as the critical adhesive length [8] after which the strain is independent of the material transition. The comparision of the strain values along the transition in Figure 9c also shows that the angle of the metal sheet reduces the constant strain far off. This is especially remarkable since the adhesive surface of the smaller angles is bigger due to the fixed overlap length.

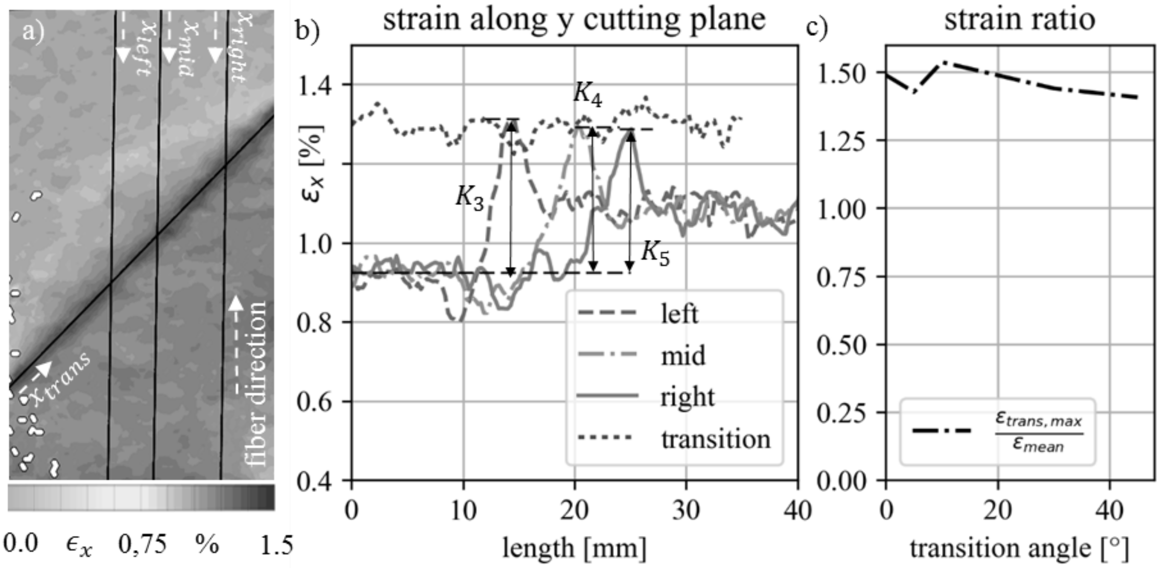

Figure 8: a) Strain distribution near the material transition with a continuous top layer (type C) b) strain along the evaluation lines c) Influence of the transition angle on the strain ratio between the mean strain before and the maximum in the transition for specimen type C measured by DIC.

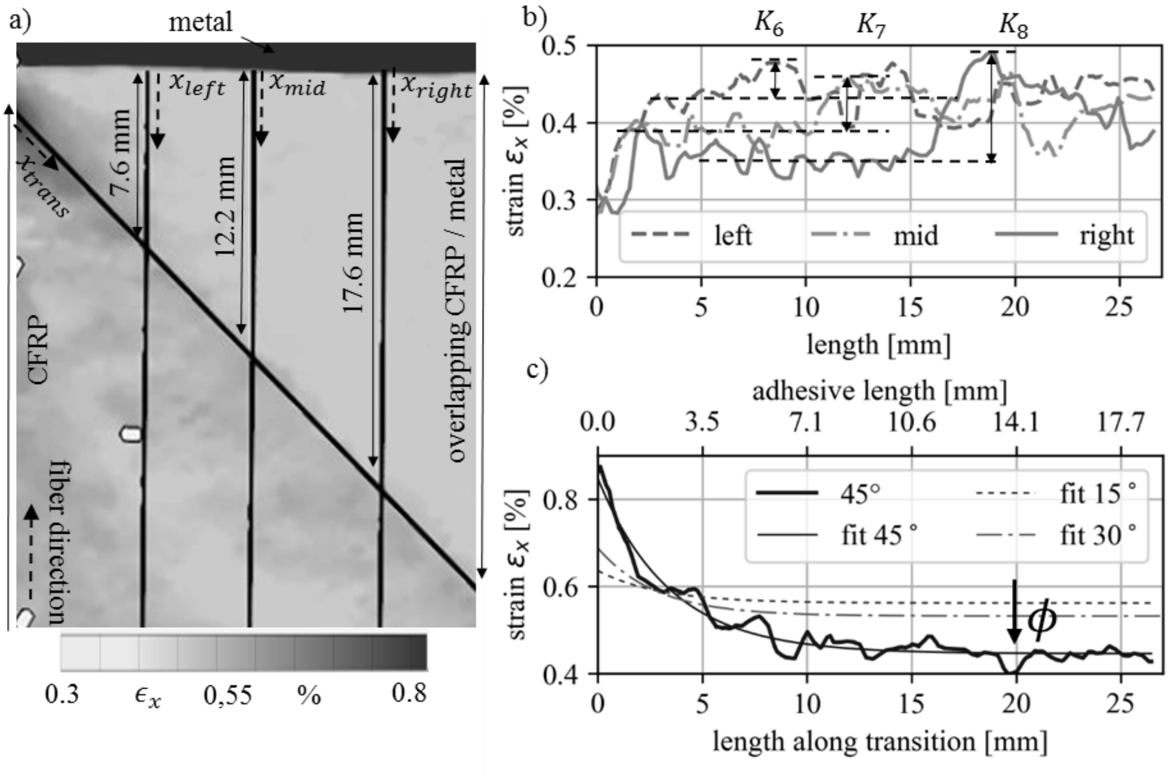

Figure 9: a) Strain distribution ϵ_x near the material transition b) strain along the evaluation lines c) comparison of the strain values along the transition for different angles ϕ.

Conclusion & Outlook

It could be shown that, the measured strain values (by DIC) and the predicted strain values of the FE-model match very well for very thin CFRP and hybrid double-lap joints. In case of a continuous CFRP layer on top and below the material transition, the strain values are constant along the transition and nearly independent of its angle. The proportionality of the strain to $cos(\phi)$ could not be observed. Therefore, 2D analytical and 2D FE models can be used to describe this section in the transmission load case. In case of a disturbed top and bottom layer the critical adhesive length has to be taken into account as well as the dependence between the transition angle and the minimal strain, which is reduced by increasing the transition angle. Currently the simplified models underestimate the strain ratio in case of type C by 16 % while overestimating type D by 21 % which has to be addressed in further investigations.

Acknowledgements
This paper is based on investigations of the subproject 1 – ‘Multilayer Inserts – intrinsic hybrid compounds for load introduction into thin walled high-performance CFRP-Structures’ of the priority program 1712 ‘Intrinsic hybrid composites for lightweight load-bearings’, which is kindly supported by the German Research Foundation (DFG).

References

[1] Schmidt C, Denkena B, Gross L, Völtzer K. Concept for Automated Production of CFRP-metal Hybrid Compounds Integrated in an Automated Fiber Placement Process. Procedia 5CIRP6 2017;62:56–61.

[2] Groß L, Herwig A, Berg DC, Schmidt C, Denkena B, Horst P et al. Production-based design of a hybrid load introduction element for thin-walled CFRP Structures. Prod. Eng. Res. Devel. 2018;12(2):113–20.

[3] Banea MD, da Silva LFM. Adhesively bonded joints in composite materials: An overview. Proceedings of the Institution of Mechanical Engineers, Part L: Journal of Materials: Design and Applications 2009;223(1):1–18.

[4] Volkersen O. Die Schubkraftverteilung in Leim-, Niet-und Bolzenverbindungen. Energie und Technik 1953;5(3,5,7).

[5] Tsai MY, Oplinger DW, Morton J. Improved theoretical solutions for adhesive lap joints. International Journal of Solids and Structures 1998;35(12):1163–85.

[6] Goland M, Reissner E. The stresses in cemented joints. Journal of Applied Mechanics 1944;11(1):A17-A27.

[7] Gültekin K, Akpinar S, Özel A. The effect of the adherend width on the strength of adhesively bonded single-lap joint: Experimental and numerical analysis. Composites Part B: Engineering 2014;60(Supplement C):736–45.

[8] Schürmann H. Konstruieren mit Faser-Kunststoff-Verbunden. Springer-Verlag Berlin Heidelberg 2007.

[9] Katnam KB, Da Silva LFM, Young TM. Bonded repair of composite aircraft structures: A review of scientific challenges and opportunities. Progress in Aerospace Sciences 2013;61:26–42.